

# Preparation of protein nanocrystals and their characterization by solid state NMR

Rachel W. Martin and Kurt W. Zilm\*

*Department of Chemistry, Yale University, P.O. Box 208107, New Haven, CT 06520-8107, USA*

Received 24 June 2003; revised 24 June 2003

## Abstract

Preparation of proteins in their crystalline state has been found to be important in producing stable therapeutic protein formulations, cross-linked enzyme crystals for application in industrial processes, generating novel porous media for separations, and of course in structure elucidation. Of these applications only X-ray crystallography requires large crystals, defined here as being crystals 100s of microns or greater in size. Smaller crystals have attractive attributes in many instances, and are just as useful in structure determination by solid state NMR (ssNMR) as are large crystals. In this paper we outline a simple set of procedures for preparing nanocrystalline protein samples for ssNMR or other applications and describe the characterization of their crystallinity by ssNMR and X-ray powder diffraction. The approach is demonstrated in application to five different proteins: ubiquitin, lysozyme, ribonuclease A, streptavidin, and cytochrome *c*. In all instances the nanocrystals produced are found to be highly crystalline as judged by natural abundance  $^{13}\text{C}$  ssNMR and optical and electron microscopy. We show for ubiquitin that nanocrystals prepared by rapid batch crystallization yield equivalent  $^{13}\text{C}$  ssNMR spectra to those of larger X-ray diffraction quality crystals. Single crystal and powder X-ray diffraction measurements are made to compare the degree of order present in polycrystalline, nanocrystalline, and lyophilized ubiquitin. Solid state  $^{13}\text{C}$  NMR is also used to show that ubiquitin nanocrystals are thermally robust, giving no indication of loss of local order after repeated temperature cycling between liquid nitrogen and room temperature. The methods developed are rapid and should scale well from the tenths of milligram to multi-gram scales, and as such should find wide utility in the preparation of protein nanocrystals for applications in catalysis, separations, and especially in sample preparation for structural studies using ssNMR.

© 2003 Elsevier Inc. All rights reserved.

**Keywords:** Solid state NMR; Protein crystallization; Protein crystals; Glass transition temperature;  $^{13}\text{C}$  NMR; Protein powder diffraction

## 1. Introduction

Every student of chemistry learns that crystallization is the most rudimentary of laboratory techniques for isolating and purifying simple organic molecules. At the same time, crystallization of large proteins or other macromolecules is viewed as a form of biochemical high art; difficult, unpredictable, and not to be ventured by the easily frustrated. This perception has largely relegated crystallization of macromolecules to the domain of structural biology laboratories focused on X-ray crystallography, where the emphasis is on producing small numbers of large defect free crystals. Protein

purification and isolation usually involves chromatography, dialysis or centrifugation, and lyophilization, but rarely a crystallization step [1]. When supplied in solid form, commercially available proteins are almost always offered as lyophilized powders.

An increasingly large body of research is finding that crystalline forms of enzymes and other proteins have substantive advantages over amorphous lyophilized powders [2–4]. The bioavailability and stability of relatively small organics used as pharmaceuticals as a rule is dependent on crystal form. In a similar fashion, the kinetics of dissolution of protein crystals depends on crystal form, and crystals are found to have higher inherent stability than amorphous powders. Crystalline enzymes are also found to have higher activity than amorphous preparations [5–7]. Stabilization of enzyme

\* Corresponding author. Fax: 1-203-432-6144.

E-mail address: [kurt.zilm@yale.edu](mailto:kurt.zilm@yale.edu) (K.W. Zilm).

crystals by chemical cross-linking provides superior stability, making the application of enzyme catalysis in industrial processes a reality [8–10]. The wide variety of molecular topologies found in macromolecular crystals makes them a novel class of mesoporous materials [11], and at the unit cell level can be viewed as biochemical cousins of zeolites and silica-alumina-phosphates. In these types of applications much smaller crystals than would be used in X-ray studies may be preferred to maximize the surface area to volume ratio while preserving crystal habit [12].

Crystalline preparations also have inherent advantages for structural studies using solid state NMR (ssNMR). As in solution-state NMR of biological macromolecules, resonance assignment of uniformly isotopically enriched molecules by homonuclear and heteronuclear chemical shift correlation is a prerequisite for determination of structure and dynamics. Unfortunately the chemical shift resolution [13] that can be obtained using the most readily accessible solid form of most proteins, lyophilized powder, is insufficient for large conformationally rich molecular systems. This is simply a result of the well-known fact that chemical shifts are sensitive to molecular conformation, which quite generally results in  $^{13}\text{C}$  linewidths of 1–2 ppm for samples that can be described as glassy. Although the proteins in a lyophilized powder might be properly folded, it is to be expected that the conformation of side chains will be quite variable. Each molecule then will have a slightly different shift for each chemically equivalent site because they are rendered magnetically inequivalent by this structural heterogeneity. Linewidths for lyophilized proteins are typically not narrow enough to provide for resolution of single sites by NMR spectroscopy.

One strategy in ssNMR studies for dealing with the structural heterogeneity of lyophilized enzymes and other proteins has been to use selective isotopic labeling. This approach provides unambiguous resonance assignment and facilitates very accurate measurement of particular distances and angles in spin pair labeled molecules [14,15]. Local conformational homogeneity is not so critical as the small number of labeled sites does not require high spectral resolution. Such experiments depend upon preparation of a selectively labeled sample, and provide only a limited number of structural constraints. While providing a powerful structural probe for specific problems, the limited applicability of the approach and the desire to utilize uniform isotopic enrichment as is standard in solution macromolecular NMR makes development of alternative methods desirable.

Significant effort has been expended on improving the resolution of ssNMR spectra for lyophilized samples by use of structure and hydration stabilizing additives. Enhanced resolution in the  $^{31}\text{P}$  NMR spectrum has been

observed for ligands bound to the enzyme 5-enolpyruvyl-shikimate-3-phosphate in lyophilized preparations protected by the addition of trehalose and polyethylene glycol (PEG) prior to lyophilization [13]. Trehalose has been used as a protectant against dehydration [16] since it was discovered that organisms adapted to very dry conditions contain high concentrations of this carbohydrate [17]. The conformation and mobility of dehydrated proteins with and without these additives has been studied by ssNMR [18–21] and by X-ray diffraction [22–24]. For most proteins, keeping samples hydrated is found to do a better job of preserving native structure and retention of activity in the solid state, and provides higher resolution NMR spectra than lyophilization without such precautions. Unfortunately no procedure for preparing protein samples for ssNMR investigations had been discovered which results in resolution comparable to that obtained on crystalline material.

Multidimensional NMR methods can also be employed to improve resolution of complex spectra, and using uniform isotopic enrichment of  $^{13}\text{C}$  or  $^{15}\text{N}$  these methods facilitate sequential assignments for the resonances in proteins. Numerous such methods have been demonstrated on model peptides [25,26] and proteins [27–30]. These studies have shown that 2D and 3D ssNMR can pull apart the myriad of resonances encountered in a protein, just as in solution NMR. Backbone and side chain  $^{13}\text{C}$ ,  $^{15}\text{N}$ , and possibly even  $^1\text{H}$  resonances [31] can be correlated and assigned in multidimensional experiments as the first step in the structure determination of an entire protein in the solid state by NMR. However, in order to perform reliable assignments, the spectral resolution must be high enough to provide for a high percentage of resolvable single sites. Single site resolution for a majority of the expected resonances in 2D NMR spectra has only been demonstrated for two small proteins [28,30] in microcrystalline form; bovine pancreatic trypsin inhibitor (BPTI) and the SH3 domain from  $\alpha$ -spectrin. Resolution has been critically compared for SH3 samples prepared by lyophilization with and without rehydration or protection with PEG and sucrose, and precipitation with ammonium sulfate [32]. The hydrated microcrystalline precipitate yielded the best  $^{13}\text{C}$  spectral resolution of the samples examined, with linewidths comparable to those typical of small crystalline model compounds. Even using multidimensional NMR methods, lyophilization has not been found to provide sufficiently narrow lines.

In this paper we more generally investigate the crystallinity requirements for achieving high resolution ssNMR spectra by studying a variety of proteins, and describe a method for rapidly producing suitable samples. Natural abundance  $^{13}\text{C}$  cross-polarization magic angle spinning (CPMAS) NMR spectra of protein taken for X-ray quality crystals and what we term

nanocrystalline precipitates are shown to be essentially identical and highly resolved, while those for lyophilized materials give poor resolution. The nanocrystalline materials are produced by a rapid bulk crystallization method in which precipitation conditions [33,34] found in an initial screening are scaled up using a centrifugal evaporator. This approach has been applied to five different proteins that have been previously characterized by single crystal X-ray diffraction. In the instance of ubiquitin a new crystal polymorph was discovered. The bulk crystallization method is easily scaled from the  $10^{-3}$  to the  $10^2$  ml scale, and can be performed to provide for essentially quantitative recovery of limited protein as crystalline solid.

In addition to being a convenient route to crystalline protein samples for ssNMR, the technique can be used for rapid preparation of bulk protein nanocrystals for other applications. These nanocrystalline precipitates are further characterized by powder X-ray diffraction, as well technique, as well as by optical and scanning electron microscopy. Protein precipitates formed in this manner are shown to consist of crystals tens of nanometers across, having the same morphology as large crystals prepared much more slowly using the same crystallization conditions. While these nanocrystals are not useful in X-ray structure determination, they potentially can be grown larger in size by Ostwald ripening [35] or serve as seeds. More importantly, nanocrystalline protein preparations can be worked up from stock solutions in less than an hour, as opposed to the days or weeks commonly used in evaporative bulk crystallizations [36]. Their ease of preparation in combination with the small size of the crystals makes this crystallization approach attractive in chemical applications of protein crystals to catalysis and separations.

Solid state  $^{13}\text{C}$  NMR of natural abundance protein samples is shown to be a sensitive indicator of their crystallinity. Solid state NMR then should prove a useful analytical tool for investigating the crystallinity of all sorts of chemically important protein preparations not amenable to X-ray methods, in direct parallel with the important role ssNMR already plays in characterizing polymorphism and other aspects of solid state structure in pharmaceutical preparations [37–39].

## 2. Materials and methods

### 2.1. Preparation of protein samples

Samples of ubiquitin, lysozyme, ribonuclease A, and cytochrome *c* used in this study were purchased from Sigma. Streptavidin was purchased from CalBioChem. Crystallization conditions were screened by the hanging drop method with 4  $\mu\text{l}$  drops containing a 1:1 mixture of protein stock solution and crystallization solution [40].

Each drop was equilibrated against 0.75 ml of crystallization solution. Crystal trays were incubated at 4 °C, except for streptavidin, which was kept at room temperature. For the ubiquitin samples, large crystals formed in approximately 2 weeks. For the lysozyme, RNase A and cytochrome *c* samples, formation of small crystals occurred in 1–2 days, with larger lysozyme crystals appearing within several days. Crystal formation occurred in the streptavidin sample within a few minutes, with the growth of larger crystals over a week.

In all screening experiments, it was observed that higher concentrations of protein, precipitating agent, or salt produced many small crystals quickly, whereas lower concentrations produced larger crystals over a longer period of time. This principle has been previously shown using a variety of proteins, salts, and precipitating agents [41–47]. Polyethylene glycol (PEG) was used here as a precipitating agent in all of the crystallization screens because of its demonstrated utility for the crystallization of proteins at low ionic strength [48–50].

Nanocrystalline samples were produced starting with stock solution prepared from 10 mg of protein. A typical sample preparation took less than one hour. Crystallization solutions for making these bulk preparations were made using the components found to produce large crystals in initial screening trays. Equal amounts of protein stock solution and crystallization solution were combined and the resulting solution was concentrated to approximately half the starting volume by vacuum over a period of 15–40 min at approximately 25 °C using a centrifugal evaporator (Savant SpeedVac). This technique is equivalent to a vapor diffusion experiment in which the well solution is twice the concentration of the drop solution in all components. Speeding the process up of course results in smaller crystals. Hydrated samples were packed in 2.5 mm zirconia rotors (Varian Inc.) by centrifugation and the supernatant was decanted. Kel-F spacers fitted with fluorosilicon o-rings (Apple Rubber) were used on each side of the sample in order to maintain hydration throughout the experiment.

### 2.2. X-ray crystallography

Single crystals were mounted in 0.5 mm diameter quartz capillaries and single crystal diffraction experiments were performed at room temperature to verify unit cell parameters, or in the case of ubiquitin determine them for the new polymorph produced. A copper  $\text{K}_\alpha$  rotating anode source with a MAR 345 image plate detector was used for data collection. About 30–45 frames were collected for each crystal with an exposure time of 10 min per frame. Analysis of the single crystal X-ray data was performed using the software package HKL 2000 [51,52].

Standard powder XRD instruments require fairly large samples, and do not easily provide for keeping

powdered samples hydrated. To characterize the crystal form of the protein nanocrystals being studied, we instead used the image plate equipped single crystal diffractometer described above. Powder XRD data collection was carried out at 100 K using  $\sim 6 \mu\text{l}$  of sample frozen in a 0.25 mm nylon loop. The polycrystalline and nanocrystalline samples were frozen as a hydrated slurry of material. Lyophilized ubiquitin was placed on the loop without rehydration. A single frame with a four hour exposure time was collected for each sample. Analysis of the powder diffraction data was performed using the program FIT2D [53,54], and the data indexed using the known positions for ice rings.

### 2.3. NMR spectroscopy

$^{13}\text{C}$  NMR spectra were collected at 18.8 T using a Varian Inova 800 MHz ( $^1\text{H}$  Larmor frequency) spectrometer at 201.1 MHz using a homebuilt triple resonance MAS probe with variable temperature capability [55]. All spectra were obtained using a cross-polarization (CP) sequence with a 10% linear ramp on the proton CP level and a 2 ms CP mixing time. A 140 kHz proton decoupling field with TPPM modulation [56] was used during the 20 ms acquisition time. Spectra were recorded with 2048 complex points at a spectral width of 100 kHz and the carrier placed between 118 and 125 ppm. A recycle delay of 3 s was used in all experiments with a spinning speed of approximately 14.5 kHz. Ubiquitin spectra (8451 Da MW) were signal averaged to 30 000 scans; while lysozyme spectra (14 100 Da MW) were averaged to 70 000; cytochrome *c* (12 400 Da MW) to 42 500; streptavidin (56 000 Da MW, 14 000 per monomer) to 77 500 and RNase A (13 700 Da MW) to 100 000. More scans were collected on the larger proteins in order to achieve comparable signal to noise for single sites. Sample temperature was controlled using a stream of dry nitrogen gas cooled to between  $-4$  and  $-120^\circ\text{C}$  delivered via a glass dewar to the spinning sample as described elsewhere [55]. Chemical shifts were referenced to external adamantane [57].

## 3. Results

### 3.1. Ubiquitin: polycrystalline, nanocrystalline, and lyophilized samples

A sitting drop screen with 25  $\mu\text{l}$  drops (12.5  $\mu\text{l}$  of stock solution and 12.5  $\mu\text{l}$  well solution) was performed in order to assess the best conditions for making a large quantity of moderate sized crystals for a polycrystalline ssNMR sample. Twenty five percentage PEG 8000 as a 25% solution on a weight per volume (w/v) basis was used throughout, and the cadmium acetate, concentration varied from 200 to 0.8 mM. Two hundred

millimolar cadmium acetate produced plentiful crystals of moderate size ( $\sim 0.2$  mm across) and this concentration was chosen for the production of the NMR sample. A polycrystalline sample of ubiquitin at pH 7 was prepared by collecting crystals from thirty 25  $\mu\text{l}$  sitting drops using a crystallization solution 25% w/v PEG 2000, 200 mM in cadmium acetate, and 50 mM in sodium Hepes buffer (pH 7). The protein stock solution contained 25 mg ubiquitin per ml of water. A photograph of representative crystals from this sample is shown in Fig. 1a. The crystals average  $\sim 200 \mu\text{m}$  across. They are cubic in appearance and not birefringent. X-ray diffraction data was collected on single crystals from this batch, and the lattice type was found to be primitive cubic with unit cell dimensions  $a = b = c = 106.45 \text{ \AA}$ . This crystal form differs from the reported structure, which formed rectangular prisms in the orthorhombic space group  $P2_12_12_1$  and unit cell dimensions  $a = 50.73 \text{ \AA}$ ,  $b = 42.75 \text{ \AA}$ , and  $c = 28.78 \text{ \AA}$ . This latter form has one molecule in the asymmetric unit [58,59]. The original literature reported crystallization was carried out by equilibrating a 5  $\mu\text{l}$  drop of 25 mg/ml ubiquitin against a solution containing 28% w/v PEG 4000 in 0.05 M cacodylate buffer at pH 5.6. This produced plate-like crystals in about 6 weeks. Comparable crystals were reported to only be produced by seeding with material from the original preparation [60].

Approximately 6.5 mg of crystals from our conditions were collected from the sitting drops and packed into a 2.5 mm rotor. The solid state  $^{13}\text{C}$  MAS NMR spectrum of these crystals is shown in Fig. 1b. The resonances at  $\sim 7.0$  and 7.5 ppm have been tentatively assigned to a pair of Ile methyl groups by comparison to the solution NMR  $^{13}\text{C}$  chemical shifts. The linewidths of these resonances are around 40 Hz, i.e.,  $\sim 0.2$  ppm.

A nanocrystalline sample was prepared by starting with the same initial conditions used in the production of the polycrystalline sample by vapor diffusion, and concentrating the solution to twice the initial concentration of all components over a period of approximately 20 min using a centrifugal evaporator (Savant SpeedVac). A photograph of crystals from this sample is shown in Fig. 1c. These crystals average less than a micron in size, much too small for use in single crystal X-ray diffraction studies. To confirm that the morphology of this precipitate was the same as that of the X-ray quality crystals, the precipitate was studied using scanning electron microscopy. Samples were prepared by evaporation of nanocrystal containing solutions onto glass slides. The slides were then coated with gold and imaged using a JEOL JXA-8600 scanning electron microscope with an accelerating voltage of 15 kV and an emission current of 2–10 nAmps.

Obtaining useful images required several attempts. In most cases the crystals violently fragmented when the sample chamber was evacuated, but on occasion islands

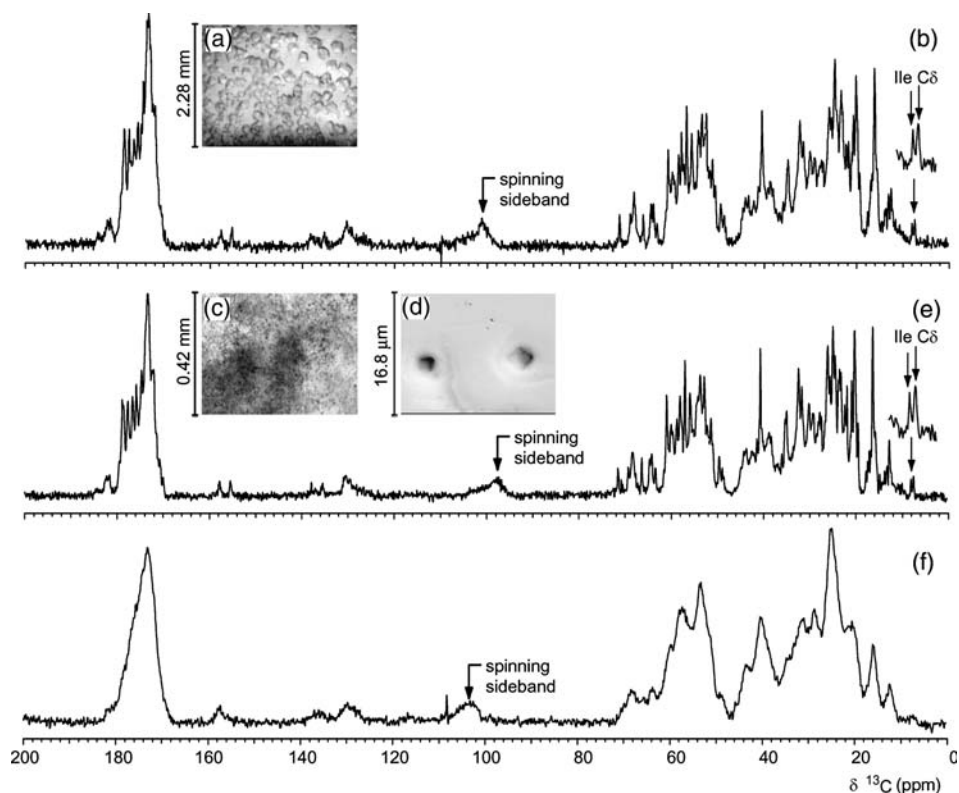


Fig. 1. (a) Ubiquitin crystals grown in a sitting drop photographed at  $5\times$  magnification using a light microscope and a Polaroid camera. The crystals measure approximately  $200\mu\text{m}$  across the widest point of an average crystal. (b) Solid state  $^{13}\text{C}$  spectrum of a polycrystalline sample composed of crystals grown using the same conditions. (c) Nanocrystals produced using rapid batch crystallization with starting conditions as in the sitting drop well of (a) photographed at  $225\times$  magnification using a light microscope and a digital camera. The morphology of individual crystallites is difficult to distinguish using the available magnification. (d) An electron micrograph of the same sample taken at  $4000\times$  magnification, showing larger than average nanocrystals, have the same cubic morphology as the larger crystals. (e) The solid state  $^{13}\text{C}$  NMR spectrum of the nanocrystals looks practically identical to that of the polycrystalline sample. (f) The  $^{13}\text{C}$  solid state spectrum of lyophilized ubiquitin is poorly resolved, indicating structural heterogeneity in the sample.

of crystals froze or otherwise were stabilized rapidly enough on the sample stage to survive evacuation of the sample chamber. A scanning electron micrograph obtained in one of these successful attempts is shown in Fig. 1d. The two crystals easily seen are  $\sim 10\times$  larger than the average crystal, some of which are seen as specks in this view. While the majority of the crystals are too small for their shapes to be readily recognized, we assume that they have the same crystal habit as displayed by these larger members of the sample. These latter crystals are  $1\text{--}2\mu\text{m}$  in dimension, while the bulk of the precipitate is comprised of crystals the order of  $100\text{nm}$  on a side. For this particular protein these dimensions correspond to crystallites containing a few thousand unit cells. The ssNMR spectrum of this nanocrystalline sample is shown in Fig. 1e. This spectrum is practically identical to that of the sample consisting of larger crystals. The linewidths of the Ile methyl groups are again around  $0.2\text{ppm}$ .

Since the ssNMR spectra of the polycrystalline and nanocrystalline samples are effectively indistinguishable, powder X-ray diffraction studies were performed on these samples in order to further assess their crystal-

linity and to determine if both preparations contain crystals with the same symmetry and unit cell dimensions. The powder diffraction pattern of the polycrystalline ubiquitin sample is shown in Fig. 2a. Numerical integration of the image plate intensities [53,54] provides the corresponding diffractogram in Fig. 2b. The pattern shows two strong rings at low resolution ( $\sim 74$  and  $\sim 37\text{\AA}$ ), as well as a slightly less intense one at  $\sim 23\text{\AA}$ . Individual spots can be seen on the rings, indicating that this sample still contains a mixture of large and small crystallites. This demonstrates that although the sample has been packed into the rotor, removed, and then frozen onto a nylon loop for the powder diffraction study, that it is still largely comprised of polycrystalline material.

The powder diffraction pattern (Fig. 2c) and diffractogram (Fig. 2d) for the nanocrystalline sample show the same strong rings at low resolution, indicating that the unit cell is the same. The rings at intermediate resolution are similar, but individual spots cannot be seen, revealing the lack of large crystals in the sample. The powder diffraction pattern and diffractogram of lyophilized ubiquitin are shown in Figs. 2e and f, respectively.

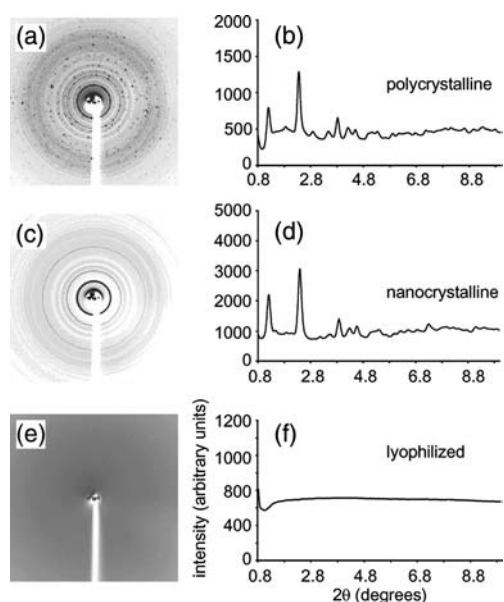


Fig. 2. Powder diffraction pattern and the corresponding diffractogram shown for polycrystalline ubiquitin in (a) and (b). The same data for the nanocrystalline sample is shown in (c) and (d) and for lyophilized ubiquitin in (e) and (f).

No diffraction spots or rings are apparent for this sample, indicating that it is completely disordered. The corresponding ssNMR spectrum is shown in Fig. 1f. Only resonances corresponding to types of chemical groups are resolved, with no distinct chemical sites, confirming that the sample has a high degree of structural heterogeneity.

### 3.2. Lysozyme, streptavidin, ribonuclease A, and cytochrome c

Crystals of lysozyme were grown according to a variation of a published method [61]. Crystallization of lysozyme is typically performed at pH 4.6 using sodium acetate as the buffer and sodium chloride as the precipitant. This protocol was modified by reducing the concentration of sodium chloride and adding PEG 2000 as an additional precipitating agent. Protein was dissolved in 100 mM sodium acetate at pH 4.5 to form a stock solution at 25 mg/ml. The screen was performed at pH 4.5 using 200 mM sodium acetate as the buffer. The amount of PEG 2000 was held constant at 50% w/v and the concentration of sodium chloride was varied from 7.5 to 67.5 mM. A photograph of crystals from the hanging drop screen is shown in Fig. 3a. Crystals from this screen were used to collect single crystal X-ray diffraction data. The lysozyme crystals were found to have unit cell dimensions  $a = b = 79.15 \text{ \AA}$  and  $c = 38.06 \text{ \AA}$ , consistent with the common tetragonal form of lysozyme belonging to the space group  $P4_32_12$  [62]. Nanocrystals produced using a crystallization solution 12.5% w/v PEG 2000, 75 mM in NaCl, and 100 mM in pH 4.5

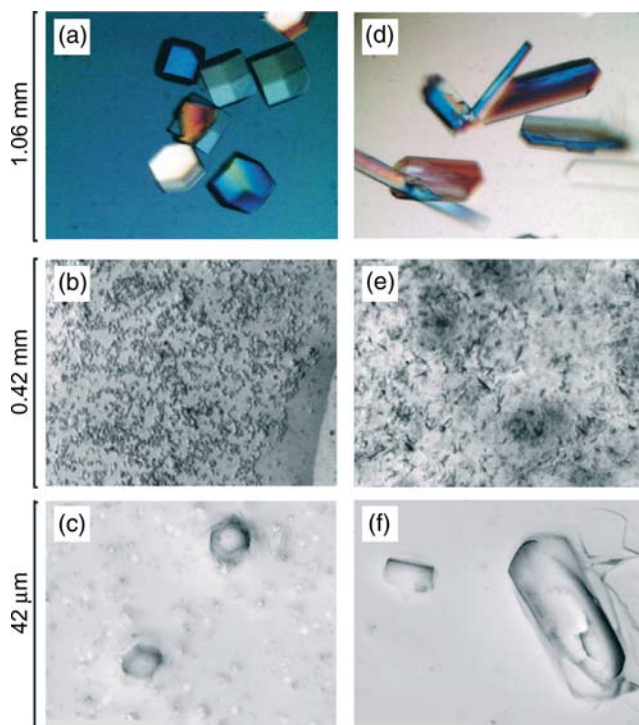


Fig. 3. Photos of other protein crystals studied. Left lysozyme (a–c) and right streptavidin (d–f). The top row shows large crystals produced in a hanging drop screen photographed using a light microscope with a polarizing filter at  $90\times$ . The middle row of photos shows nanocrystals produced using the same starting conditions as those used in the well solutions of the hanging drop screens for (c) lysozyme and (d) streptavidin. The nanocrystals were photographed using a light microscope at  $225\times$  magnification. The overall morphology of the crystallites can be seen to match with that of the larger crystals in each case. The bottom figures show electron micrographs of the same nanocrystals, at  $2200\times$  magnification. Micrographs shown are for larger than representative crystals as discussed in the text.

sodium acetate buffer, are pictured in Fig. 3b. An electron micrograph of the nanocrystals is shown in Fig. 3c. This was acquired as described for the ubiquitin nanocrystals. Once again a pair of larger crystals has been chosen to demonstrate that the crystal morphology produced is the same as obtained under conditions more conducive to producing diffraction quality crystals. The much smaller crystals, providing the speckled background in Fig. 3c, are representative of the average crystal produced by rapid centrifugal concentration. A ssNMR  $^{13}\text{C}$  spectrum of the nanocrystalline sample is shown in Fig. 4a. Some assignments can be made from this spectrum based on a previously published solution spectrum [63]. Several residues in the aromatic region of the spectrum can be specifically assigned, and others can be identified by type of residue. In particular we note the  $\delta$ -methyl resonance for Ile 28 as indicated in the figure. This resonance is for a single carbon center in this protein, and is readily identified by its unusual chemical shift upfield of tetramethylsilane. Apparently the tertiary structural features that result in this unusual highly

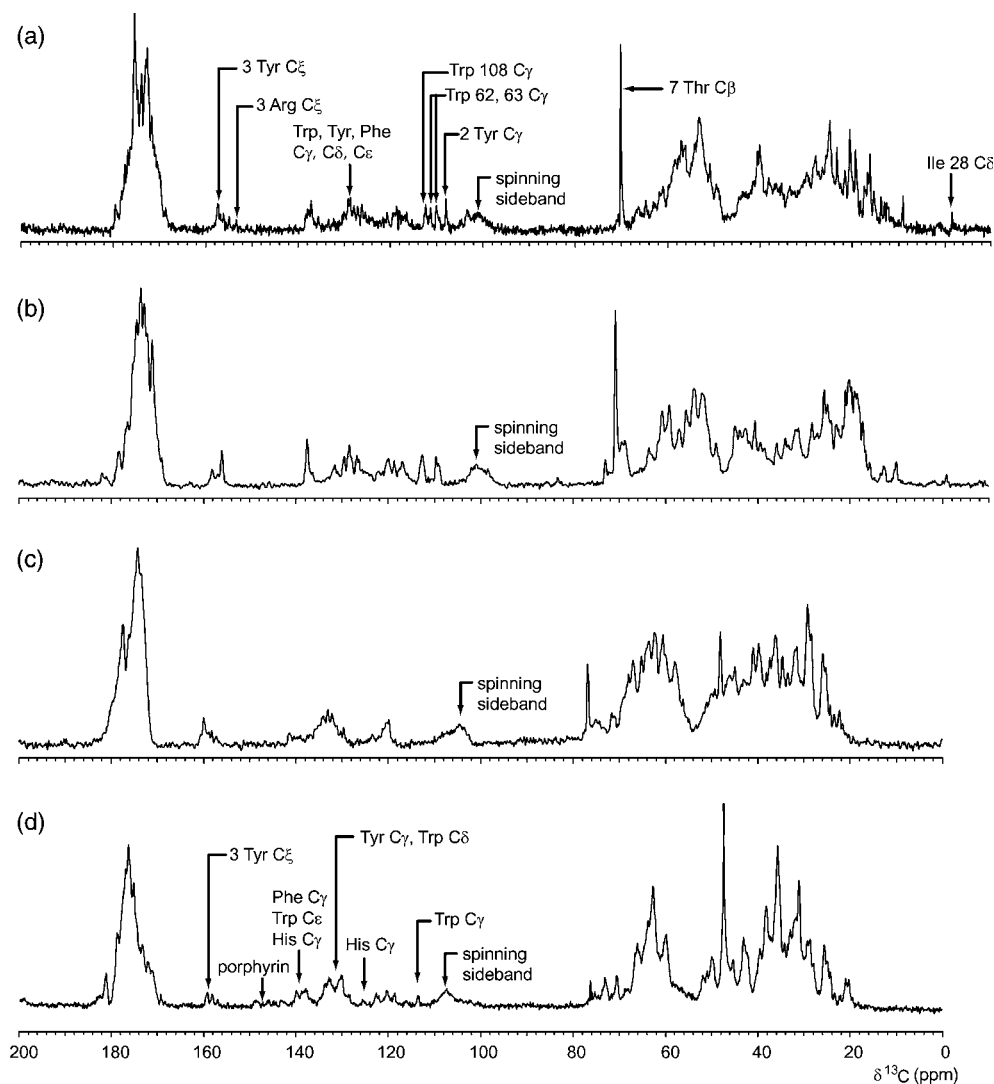


Fig. 4.  $^{13}\text{C}$  ssNMR spectra of nanocrystalline proteins. (a) Lysozyme, (b) streptavidin, (c) ribonuclease A, and (d) cytochrome *c*. Partial assignments have been made based on previously published  $^{13}\text{C}$  solution state NMR data as indicated where they are available.

shielded  $^{13}\text{C}$  shift in solution are the same as those in the solid state.

The crystallization protocol used for streptavidin was adapted from published conditions using sodium chloride and ammonium sulfate at pH 4.6 [64]. In this study, the same pH was used but PEG 2000 was used in place of ammonium sulfate. The screening solutions contained 50 mM sodium acetate at pH 4.5 as well as 200 mM NaCl. The concentration of PEG 2000 was varied from 2.5 to 45% w/v. Crystals of streptavidin formed very rapidly, with hanging drops having a high concentration of precipitant producing crystals within minutes and larger ones appearing overnight.

Crystals from this screen are pictured in Fig. 3d. The corresponding nanocrystals, which have the same plate-like shape, are shown in Fig. 3e and in the scanning electron micrograph in 3f (again for a much larger than representative crystal). These were prepared using a

stock solution of 12.5 mg/ml streptavidin in water, and a crystallization solution 25% by w/v PEG 2000, 200 mM in NaCl, and 50 mM in sodium acetate pH 4.5 buffer. The ssNMR spectrum of the nanocrystalline sample is shown in Fig. 4b. While the narrow features in the ssNMR  $^{13}\text{C}$  spectrum indicate that the sample is crystalline, there are fewer resonances that could tentatively be identified as belonging to a single carbon site. This undoubtedly is a result of the solid state sample being a tetramer in the crystal. On account of this there will be subtle shift differences between chemically equivalent centers in different members of the tetramer, leading to less resolution in the spectrum that might be expected for a protein of this size.

A hanging drop crystal screen based on published conditions [65] was performed on RNase A. The buffer used was 10 mM sodium citrate at pH 6.5 without additional salt, and the concentration of PEG 2000 was

varied from 2.5 to 45% w/v. The largest crystals produced by the screen were slightly larger than 1  $\mu\text{m}$  in size, clearly not large enough to perform a single crystal X-ray diffraction experiment. Nanocrystals were produced from a stock solution containing 12.5 mg RNase A per ml water, and a crystallization solution 25% w/v PEG 2000 and 10 mM in pH 6.5 sodium citrate buffer. The ssNMR spectrum for this sample is shown in Fig. 4c. The resolution observed is comparable to that collected on the other proteins studied here where larger crystals were obtained under the screening conditions used for subsequent rapid crystallization. Although larger crystals presumably could have been produced using higher salt as described elsewhere [65], our aim was to avoid salty conditions if at all possible. Although solids, crystalline proteins can prove to be quite lossy radio frequency absorbers if their solvent cavities and interstitial spaces contain highly conductive solutions of water and salts. The RNase A result is important as it demonstrates that useful ssNMR resolution can be obtained for a sample prepared using conditions that only produce nanocrystals. Although this spectrum does not have as high a resolution as observed for the other proteins studied herein, it is clearly superior to what could be obtained on the lyophilizate of even a small protein, as can be appreciated by comparison to the ubiquitin spectrum in Fig. 1f.

Crystal screens of cytochrome *c* under low salt conditions based on a published protocol [66] likewise did not produce large crystals. Nanocrystals were prepared using a cytochrome *c* stock solution at 12.5 mg/ml in water, and a crystallization solution 25% w/v PEG 2000 and 10 mM in potassium phosphate pH 7.0 buffer. The NMR spectrum of cytochrome *c* nanocrystals in the oxidized form is shown in Fig. 4d. This spectrum shows broadening of some resonances due to the presence of the paramagnetic iron, but the presence of many narrow resonances indicates that the overall structure of the protein is ordered. The aromatic region is of particular interest because some of the aromatic resonances can be assigned by analogy to the results of a previously published solution state  $^{13}\text{C}$  NMR experiment [67].

### 3.3. The effect of temperature cycling on ubiquitin nanocrystals

Crystals of biological macromolecules are often fragile with respect to temperature cycling and freeze–thawing. Crystalline samples for X-ray diffraction studies using synchrotron radiation are usually flash frozen and continuously cooled at liquid nitrogen temperature in order to provide protection from damage in the X-ray beam. Samples for these experiments generally contain a cryoprotectant such as glycerol that is co-crystallized with the protein or soaked into existing crystals [68]. Protein crystals of the size used for X-ray

diffraction are generally destroyed by repeated freeze–thawing.

For NMR studies, where the same sample is often reused for a series of measurements, such a constraint would be extremely inconvenient. In fact, the experimental hardware used in many laboratories does not provide for sample changes at low temperatures. To investigate this aspect of the interplay of sample order and ssNMR spectral resolution, spectra for a sample of nanocrystalline ubiquitin were recorded as a function of temperature and after repeated temperature cycling.

Fig. 5 displays a series of  $^{13}\text{C}$  MAS NMR spectra for ubiquitin with decreasing temperature. This sample shows little change from 3 to  $-40^\circ\text{C}$ , but at lower temperatures the effects of the freezing become apparent. Over this temperature range, the proton  $T_1$ , which was measured indirectly through the  $^{13}\text{C}$  nuclei by inversion recovery, remains constant at approximately 0.5 s. At  $-80^\circ\text{C}$  many of the protein resonances are broadened, and a sharp line begins to appear at around 70 ppm. This resonance is consistent with the chemical shift of polyethylene glycol (PEG 2000) in solution and is not observed at higher temperatures. Above  $-80^\circ\text{C}$  the PEG is apparently sufficiently mobile that it does not give a cross-polarization spectrum. Once the PEG begins to freeze, the  $^{13}\text{C}$ – $^1\text{H}$  dipolar interactions are no longer motionally averaged away, making it possible for the  $^{13}\text{C}$  nuclei in the PEG to be cross polarized and appear in the CPMAS spectrum. At  $-120^\circ\text{C}$ , the PEG line increases in intensity and further broadening of the protein spectrum occurs. At this temperature, the proton  $T_1$  of the bulk sample is longer, around 1.4 s. The bottom trace in Fig. 5 shows a spectrum for another sample at  $-40^\circ\text{C}$  after 10 freeze–thaw cycles where the sample was frozen each time by immersion in liquid nitrogen. The observation that the highly resolved  $^{13}\text{C}$  spectrum returns once the sample is equilibrated back to  $-40^\circ\text{C}$  is important. It demonstrates that the local order present in the nanocrystalline preparations that is a prerequisite for obtaining high resolution in the  $^{13}\text{C}$  ssNMR spectrum, is not damaged by repeated cycling of the sample between ambient and cryogenic temperatures. If the crystals were irreversibly disrupted or the protein cold-denatured by this treatment, the spectral resolution obtained at and above  $-40^\circ\text{C}$  would not be expected to return after the sample had been held at 77 K for any period of time. While not shown in this figure, it has been verified that the resolution also returns to the spectrum at  $-40^\circ\text{C}$  for a sample that had been held for over 24 h at  $-120^\circ\text{C}$ .

## 4. Discussion

For all the proteins studied in this work, easily prepared nanocrystalline precipitates give  $^{13}\text{C}$  ssNMR



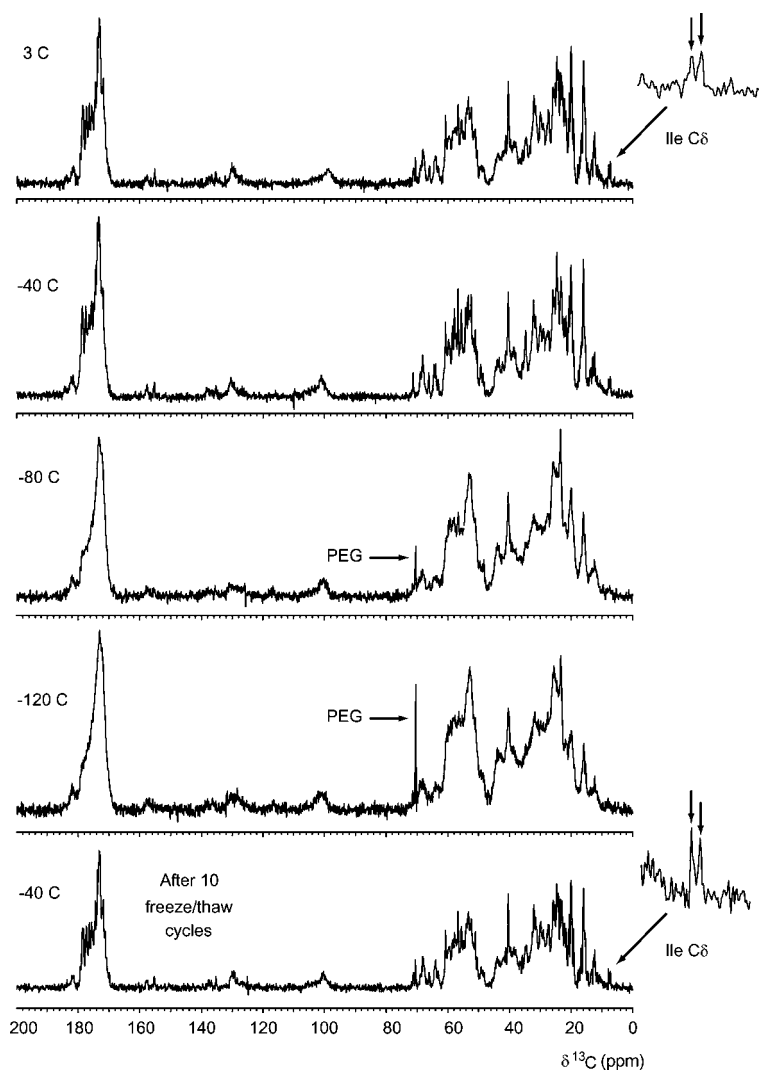


Fig. 5. Series of  $^{13}\text{C}$  ssNMR spectra of nanocrystalline ubiquitin as a function of decreasing temperature. The spectrum shows little change between 3 and  $-40^\circ\text{C}$ . At  $-80^\circ\text{C}$  the sample begins to freeze, with a PEG resonance starting to appear. This resonance becomes more pronounced at  $-120^\circ\text{C}$ , while the other spectral features continue to broaden. The bottom spectrum is for a second sample that was frozen at 77 K and warmed to room temperature 10 times before a spectrum was taken at  $-40^\circ\text{C}$ . The  $^{13}\text{C}$  resonances corresponding to a pair of Ile methyl groups are enlarged and shown as insets. These narrow features in the spectra taken for samples before and after temperature cycling are a sensitive indication of sample crystallinity.

spectra with many narrow features. Where single lines can be identified the linewidths are less than 0.4 ppm, and methyl groups can be as narrow as 0.2 ppm. This is in stark contrast to lyophilized protein preparations, where the ssNMR linewidths are generally observed to be greater than 1 ppm if not significantly more. The observation that this degree of resolution can be obtained with some generality demonstrates that the application of ssNMR methods to the investigation of large molecules should not be impeded by difficulties in producing bulk samples with crystalline local-order.

The general protocol adopted here is straightforward. Just as in an X-ray crystallographic study we identify crystallization conditions using multiple well screening of hanging drops. Once appropriate conditions are

identified, precipitates can quickly be prepared on the tens of mg level starting with stock protein and crystallization solutions. The use of a centrifugal evaporator greatly speeds up the process, and at the same time concentrates the crystals for collection. Progress of the crystallization can be readily monitored by sampling supernatant and testing for protein by any of the usual colorimetric methods. As evaluated by  $^{13}\text{C}$  ssNMR, the nanocrystalline proteins produced in this fashion have order at the thousands of unit cells level that is equivalent to those one would obtain if the protein were crystallized from the same solution by the more painstaking process of slow evaporation. In cases where bulk crystals are desired for cross-linking and subsequent use as catalysts or separations media, the smaller crystals

produced in this manner may in fact be preferable due to transport considerations [12].

The high resolution observed in  $^{13}\text{C}$  ssNMR spectra for nanocrystalline proteins is a measure of the high degree of local order present in these preparations. The extreme long range order required for X-ray diffraction is not needed in MAS ssNMR studies. This was demonstrated by showing diffraction quality crystals 100s of microns in size give the same highly resolved  $^{13}\text{C}$  ssNMR spectra that crystals only 100s of nanometers in dimension do. In either case the resolution is dramatically improved in comparison to lyophilizate, which by all measures taken here is amorphous. With the demonstration that  $^{13}\text{C}$  ssNMR spectra can be obtained with reasonable averaging times on natural abundance protein samples,  $^{13}\text{C}$  ssNMR should be considered a top candidate for characterization of any solid phase protein preparation. The technique readily differentiates between ordered and amorphous protein precipitates or other preparations, and as such should prove useful in characterization of protein micro or nanocrystals prepared for pharmaceutical or chemical applications.

Sample temperature and the temperature history of a sample are important factors in determining the amount of long range order that is observed in a large protein crystal by X-ray crystallography. As demonstrated here, these factors affect ssNMR results in a very different fashion. The nanocrystalline samples produced here retain the local order needed to produce highly resolved ssNMR  $^{13}\text{C}$  spectra after repeated cycling of the temperature between ambient and cryogenic conditions. This is in distinct contrast to what is observed in X-ray crystallography where single crystal samples are routinely flash frozen and never temperature cycled for fear of shattering the crystal. Cryogenically induced stress cracking at any length scale is lethal to the success of an X-ray diffraction experiment. In contrast the ssNMR experiment is insensitive to disruption of the crystal lattice as long as the majority of unit cells remain intact. One could also argue that the nanocrystals used here will experience much less in the way of freezing induced stress simply because they are so small. On this greatly reduced length scale the lattice is more likely on to be able to accommodate the forces accompanying freezing of solvent in and around the crystals, contributing to the insensitivity of the these preparations to temperature cycling, at least as measured by  $^{13}\text{C}$  ssNMR.

The resolution observed in a ssNMR experiment is sensitive to the time averaged local order present. Again in contrast to X-ray crystallography, ssNMR finds better resolution, and by inference more uniform time averaged local order, at temperatures where the interstitial solvent is still fluid. This is inferred by the observation that the PEG associated with these crystals gives a much more intense ssNMR cross-polarization spectrum below  $-80^\circ\text{C}$ , i.e., once it has presumably become immobilized

on the time scale of the  $^{13}\text{C}$ - $^1\text{H}$  dipolar interactions. At the same time the resolution in the  $^{13}\text{C}$  spectrum of the protein is degrading. Two related factors are thought to be simultaneously at work here. One relates to the averaging effects of translational diffusion of the solvent or other fluid components such as buffer constituents. It is unlikely that these components would be ordered on the crystal lattice to the same degree as the protein itself. Therefore the distribution of environments any particular chemically distinct  $^{13}\text{C}$  site in the protein experiences can be quite inhomogeneous if these other constituents are frozen in place. The subtle shifts of the resonance positions accompanying this distribution of environments will lead to an inhomogeneous broadening of the NMR resonances. On the other hand, once the solvent and extraneous solutes are able to diffuse rapidly enough so that each chemically equivalent  $^{13}\text{C}$  site sees the same time averaged environment, such inhomogeneous broadening will be motionally averaged away. This component of the broadening is similar to that seen in MAS spectra of zeolites [69] and other porous media under some conditions. When these types of samples are dehydrated, the  $^{29}\text{Si}$  MAS NMR spectra broaden as the charge compensating cations and other guests in the lattice can no longer diffuse freely from cage to cage. Maintaining hydration, as well as keeping the temperature elevated to assist faster diffusion of these components, has been found a requirement for obtaining the highest resolution possible in MAS spectra of these complex solids. The high resolution observed here above  $-40^\circ\text{C}$  for the ubiquitin samples is undoubtedly due to translational diffusion averaging of the same type.

In addition to freezing out the mobility of the fluid components of the cavities within our protein crystals, lower temperatures impede the motional averaging of the flexible protein side chains themselves. This in and of itself would lead to line broadening, as the side chain  $^{13}\text{C}$  shifts are quite sensitive to conformation. In addition to intermediate exchange phenomena, one would expect many lines to split into several components reflecting the variety of close in energy conformations available to any particular side chain. As the interstitial components of the crystal freeze, this type of broadening will be exacerbated by the influence the frozen solvent has on the rotational potential energy curves for the different constituent side chains. Each chemically distinct site then will see a distribution of differing barriers to side chain reorganization, and ostensibly a distribution of different potential minima as well. This wealth of structural heterogeneity brought on by the freezing of the fluid components of the protein crystal lattice then will lead to an increasingly severe inhomogeneous broadening of the  $^{13}\text{C}$  resonances until at the lowest temperatures the lines will be almost as broad as one might observe in a lyophilizate. The behavior ex-

pected on this basis is just that observed, one of a gradual broadening of the line shapes as the sample “freezes” on many different levels over several decades of temperature. In a sense these NMR experiments provide a microscopic window into the protein glass transition, which is also observed to take place by other methods within the same range of temperature [70]. Further insight into this process on a residue by residue basis could be provided by ssNMR measurements as described here, but using selective isotopic enrichment, and would complement the picture of these dynamics on the molecular scale as provided by solution NMR in inverse micelles [71].

Although not investigated in this work, it is clear that similar ssNMR studies will be able to shed much light on the role that cryoprotectants play in X-ray crystallography. Cryoprotectants certainly lend mechanical and thermal stability to many protein crystal preparations, and are often thought to facilitate improved ordering of side chains at low temperatures. However, since crystallography is generally unsuited for distinguishing static from dynamic disorder, it can be difficult to infer the molecular details of how cryoprotectants impart such stability or order to any particular protein preparation using X-ray methods. Solid state NMR studies as described herein will undoubtedly prove quite informative in this regard.

## 5. Conclusions

The results presented demonstrate that nanocrystalline material far too small to be useful in X-ray diffraction studies is suitable for structural or other biophysical studies by ssNMR. Preparation of nanocrystalline precipitates requires initial screening, but conditions can be adapted from X-ray diffraction conditions if they are known. Alternatively, conditions can usually be found by buffering the protein near its isoelectric point, and using different salts combined with varying amounts of PEG or other organic precipitants. This screening procedure is similar to a standard crystal screen for macromolecular crystallography, but does not require the fine tuning needed to identify the optimal concentrations for producing large diffraction quality crystals. Bulk samples of protein nanocrystals can be prepared rapidly in a centrifugal evaporator, and should find uses in a variety of chemical applications, especially in the preparation of cross-linked protein or enzyme crystals for catalysis or chemical separations. The precipitation method used here may prove useful even for X-ray crystallography, either as a source of material for Ostwald ripening [35] to grow larger crystals, or to provide sufficient powder for solving a structure by Rietveld analysis using high resolution synchrotron X-ray powder diffraction data [72,73].

In addition to demonstrating that nanocrystalline protein provides high resolution  $^{13}\text{C}$  ssNMR spectra, the data presented here highlight the utility of  $^{13}\text{C}$  ssNMR as a tool for evaluating crystallinity of a protein preparation. Our work here used the extremely small sample volume of  $6.5\ \mu\text{l}$  to emphasize the utility of the technique in biophysical studies, and even then convincingly showed that single sites in these large molecules could be observed using natural abundance  $^{13}\text{C}$  ssNMR spectroscopy with good sensitivity. In applications to problems in pharmaceutical formulations where larger sample quantities would be available,  $^{13}\text{C}$  ssNMR has been demonstrated here to have the potential for distinguishing different polymorphs, especially if a few uniquely shielded resonances can be identified.

## Acknowledgments

The instrumentation used in this work was provided by grants from the W.M. Keck foundation and the Chemistry Research Instrumentation Facilities program of the NSF. The authors would like to thank E. Paulson and C. Morcombe for repeating the temperature cycling experiment on nanocrystalline ubiquitin. RWM would like to thank R. Batey, A. Luptak, and J. Doudna for extensive assistance in developing crystal screening protocols, J. Wang for assistance in collecting the powder X-ray diffraction data, and L. Estroff for assistance in using the scanning electron microscopy facilities.

## References

- [1] T.M. Przybycien, Protein–protein interactions as a means of purification, *Curr. Opin. Biotechnol.* 9 (1998) 164–170.
- [2] A.L. Margolin, M.A. Navia, Protein crystals as novel catalytic materials, *Angew. Chem. Int. Edit.* 40 (2001) 2205–2222.
- [3] A.M. Klibanov, Improving enzymes by using them in organic solvents, *Nature* 409 (2001) 241–246.
- [4] A. Jen, H.P. Merkle, Diamonds in the rough: protein crystals from a formulation perspective, *Pharm. Res.* 18 (2001) 1483–1488.
- [5] B. Shenoy, Y. Wang, W.Z. Shan, A.L. Margolin, Stability of crystalline proteins, *Biotechnol. Bioeng.* 73 (2001) 358–369.
- [6] A.A. Elkordy, R.T. Forbes, B.W. Barry, Integrity of crystalline lysozyme exceeds that of a spray-dried form, *Int. J. Pharm.* 247 (2002) 79–90.
- [7] J. Lalonde, Cross-linked crystals stabilise enzymes, *Manuf. Chemist* 67 (1996) 19.
- [8] M. Ayala, E. Horjales, M.A. Pickard, R. Vazquez-Duhalt, Cross-linked crystals of chloroperoxidase, *Biochem. Biophys. Res. Commun.* 295 (2002) 828–831.
- [9] M.S. Doscher, F.M. Richards, Activity of an enzyme in crystalline state—Ribonuclease S, *J. Biol. Chem.* 238 (1963) 2399.
- [10] A. Haouz, J.M. Glandieres, B. Alpert, Involvement of protein dynamics in enzyme stability—The case of glucose oxidase, *Febs Lett.* 506 (2001) 216–220.

- [11] L.Z. Vilenchik, J.P. Griffith, N. St Clair, M.A. Navia, A.L. Margolin, Protein crystals as novel microporous materials, *J. Am. Chem. Soc.* 120 (1998) 4290–4294.
- [12] W.H. Bishop, F.M. Richards, Properties of liquids in small pores—rates of diffusion of some solutes in cross-linked crystals of beta-lactoglobulin, *J. Mol. Biol.* 38 (1968) 315.
- [13] D.L. Jakeman, D.J. Mitchell, W.A. Shuttleworth, J.N.S. Evans, Effects of sample preparation conditions on biomolecular solid-state NMR lineshapes, *J. Biomol. NMR* 12 (1998) 417–421.
- [14] J.M. Griffiths, R.G. Griffin, Nuclear magnetic resonance methods for measuring dipolar couplings in rotating solids, *Anal. Chim. Acta* 283 (1993) 1081–1101.
- [15] L.M. McDowell, J. Schaefer, High-resolution NMR of biological solids, *Curr. Opin. Struct. Biol.* 6 (1996) 624–629.
- [16] D.P. Miller, R.E. Anderson, J.J. de Pablo, Stabilization of lactate dehydrogenase following freeze-thawing and vacuum-drying in the presence of trehalose and borate, *Pharm. Res.* 15 (1998) 1215–1221.
- [17] J.S. Clegg, *Comp. Biochem. Physiol.* 14 (1965) 135–143.
- [18] S. Yoshioka, Y. Aso, S. Kojima, S. Sakurai, T. Fujiwara, H. Akutsu, Molecular mobility of protein in lyophilized formulations linked to the molecular mobility of polymer excipients, as determined by high resolution C-13 solid-state NMR, *Pharm. Res.* 16 (1999) 1621–1625.
- [19] Y.H. Lam, R. Bustami, T. Phan, H.K. Chan, F. Separovic, A solid-state NMR study of protein mobility in lyophilized protein-sugar powders, *J. Pharm. Sci.* 91 (2002) 943–951.
- [20] R.B. Gregory, M. Gangoda, R.K. Gilpin, W. Su, The influence of hydration on the conformation of lysozyme studied by solid-state <sup>13</sup>C-NMR spectroscopy, *Biopolymers* 33 (1993) 513–519.
- [21] R.B. Gregory, M. Gangoda, R.K. Gilpin, W. Su, The influence of hydration on the conformation of bovine serum albumin studied by solid-state <sup>13</sup>C-NMR spectroscopy, *Biopolymers* 33 (1993) 1871–1876.
- [22] K. Madhusudan, M. Vijayan, Protein hydration and water structure: X-ray analysis of a closely packed protein crystal with very low solvent content, *Acta Crystallogr. D* 49 (1993) 234–245.
- [23] H.G. Nagendra, N. Sukumar, M. Vijayan, Role of water in plasticity, stability and action of proteins: the crystal structures of lysozyme at very low levels of hydration, *Proteins* 32 (1998) 229–240.
- [24] J.A. Bell, X-ray crystal structures of a severely desiccated protein, *Protein Sci.* 8 (1999) 2033–2040.
- [25] A. Detken, E.H. Hardy, M. Ernst, M. Kainosho, T. Kawakami, S. Aimoto, B.H. Meier, Methods for sequential resonance assignment in solid, uniformly <sup>13</sup>C, <sup>15</sup>N labelled peptides: quantification and application to antamanide, *J. Biomol. NMR* 20 (2001) 203–221.
- [26] C.M. Rienstra, M. Hohwy, M. Hong, R.G. Griffin, 2D and 3D <sup>15</sup>N–<sup>13</sup>C–<sup>13</sup>C NMR chemical shift correlation spectroscopy of solids: assignment of MAS spectra of peptides, *J. Am. Chem. Soc.* 122 (2000) 10979–10990.
- [27] S.K. Straus, T. Bremi, R.R. Ernst, Experiments and strategies for the assignment of fully <sup>13</sup>C/<sup>15</sup>N-labelled polypeptides by solid state NMR, *J. Biomol. NMR* 12 (1998) 39–50.
- [28] A. McDermott, T. Polenova, A. Bockmann, K.W. Zilm, E.K. Paulsen, R.W. Martin, G.T. Montelione, Partial NMR assignments for uniformly (<sup>13</sup>C, <sup>15</sup>N)-enriched BPTI in the solid state, *J. Biomol. NMR* 16 (2000) 209–219.
- [29] M. Hong, Resonance assignment of <sup>13</sup>C/<sup>15</sup>N labeled solid proteins by two- and three-dimensional magic-angle-spinning NMR, *J. Biomol. NMR* 15 (1999) 1–14.
- [30] J. Pauli, M. Baldus, B. van Rossum, H. de Groot, H. Oschkinat, Backbone and side-chain C-13 and N-15 signal assignments of the alpha-spectrin SH3 domain by magic angle spinning solid-state NMR at 17.6 tesla, *ChemBiochem* 2 (2001) 272–281.
- [31] B.J. van Rossum, F. Castellani, K. Rehbein, J. Pauli, H. Oschkinat, Assignments of the nonexchanging protons of the  $\alpha$ -spectrin SH3 domain by two- and three-dimensional <sup>1</sup>H–<sup>13</sup>C solid-state magic-angle spinning NMR and comparison of solution and solid-state proton chemical shifts, *ChemBiochem* 2 (2001) 906–914.
- [32] J. Pauli, B. van Rossum, H. Forster, H.J.M. de Groot, H. Oschkinat, Sample optimization and identification of signal patterns of amino acid side chains in 2D RFDR spectra of the alpha-spectrin SH3 domain, *J. Magn. Reson.* 143 (2000) 411–416.
- [33] S.N. Timasheff, T. Arakawa, Mechanism of protein precipitation and stabilization by co-solvents, *J. Cryst. Growth* 90 (1988) 39–46.
- [34] A. McPherson, Increasing the size of microcrystals by fine sampling of pH limits, *J. Appl. Crystallogr.* 28 (1995) 362–365.
- [35] J.D. Ng, B. Lorber, J. Witz, A. TheobaldDietrich, D. Kern, R. Giege, The crystallization of biological macromolecules from precipitates: evidence for Ostwald ripening, *J. Cryst. Growth* 168 (1996) 50–62.
- [36] T.S. Lee, J.D. Vaghjani, G.J. Lye, M.K. Turner, A systematic approach to the large-scale production of protein crystals, *Enzyme Microb. Technol.* 26 (2000) 582–592.
- [37] G.A. Stephenson, R.A. Forbes, S.M. Reutzel-Edens, Characterization of the solid state: quantitative issues, *Adv. Drug Delivery Rev.* 48 (2001) 67–90.
- [38] D.E. Bugay, Characterization of the solid-state: spectroscopic techniques, *Adv. Drug Delivery Rev.* 48 (2001) 43–65.
- [39] S.R. Vippagunta, H.G. Brittain, D.J. Grant, Crystalline solids, *Adv. Drug Delivery Rev.* 48 (2001) 3–26.
- [40] P.C. Weber, in: *Overview of Protein Crystallization Methods*, vol. 276, Academic Press, San Diego, 1997, pp. 13–21.
- [41] M. Ries-Kautt, A. Ducruix, in: *Inferences Drawn from Physico-chemical Studies of Crystallogenes and Precrystalline State*, vol. 276, Academic Press, San Diego, 1997, pp. 23–60.
- [42] A. McPherson, in: *Crystallization of Macromolecules: General Principles*, vol. 114, Academic Press, Orlando, 1985, pp. 112–127.
- [43] B. Cudney, S. Patel, K. Weisgraber, Y. Newhouse, A. McPherson, Screening and optimization strategies for macromolecular crystal growth, *Acta Crystallogr. D* 50 (1994) 414–423.
- [44] I. Yoshizaki, T. Sato, N. Igarashi, M. Natsuisaka, N. Tanaka, H. Komatsu, S. Yoda, Systematic analysis of supersaturation and lysozyme crystal quality, *Acta Crystallogr. D* 57 (2001) 1621–1629.
- [45] J.P. Guilloteau, M.M. Rieskautt, A.F. Ducruix, Variation of lysozyme solubility as a function of temperature in the presence of organic and inorganic salts, *J. Cryst. Growth* 122 (1992) 223–230.
- [46] S.D. Durbin, G. Feher, Crystal-growth studies of lysozyme as a model for protein crystallization, *J. Cryst. Growth* 76 (1986) 583–592.
- [47] S.B. Howard, P.J. Twigg, J.K. Baird, E.J. Meehan, The solubility of hen egg-white lysozyme, *J. Cryst. Growth* 90 (1988) 94–104.
- [48] A. McPherson, Crystallization of proteins from polyethylene glycol, *J. Biol. Chem.* 251 (1976) 6300–6303.
- [49] R. Sousa, Use of glycerol, polyols and other protein-structure stabilizing agents in protein crystallization, *Acta Crystallogr. D* 51 (1995) 271–277.
- [50] R. Sousa, in: *Using Cosolvents to Stabilize Protein Conformation for Crystallization*, vol. 276, Academic Press, San Diego, 1997, pp. 131–143.
- [51] Z. Otinowski, in: *Proceedings of the CCP4 Study Weekend (SERC Daresbury Laboratory England), Oscillation Data Reduction Program*, 1993.
- [52] XDISPLAYF Program, Purdue University, 1993.
- [53] FIT2D V9.129 Reference Manual V 3.1, ESRF, 1997.
- [54] FIT2D: An Introduction and Overview, ESRF, 1997.
- [55] R.W. Martin, E.K. Paulson, K.W. Zilm, Design of a triple resonance MAS probe for high field solid state NMR, *Rev. Sci. Instrum.* 74 (2003) 3045–3061.

- [56] A.E. Bennett, C.M. Rienstra, J.M. Griffiths, W. Zhen, P.T. Lansbury, R.G. Griffin, Homonuclear radio frequency-driven recoupling in rotating solids, *J. Chem. Phys.* 108 (1998) 9463–9479.
- [57] C.R. Morcombe, K.W. Zilm, Chemical shift referencing in MAS solid state NMR, *J. Magn. Reson.* 162 (2003) 479–486.
- [58] W.J. Cook, F.L. Suddath, C.E. Bugg, G. Goldstein, Crystallization and preliminary X-ray investigation of ubiquitin, a non-histone chromosomal protein, *J. Mol. Biol.* 130 (1979) 353–355.
- [59] S. Vijay-Kumar, C.E. Bugg, K.D. Wilkinson, W.J. Cook, Three-dimensional structure of ubiquitin at 2.8 Angstrom resolution, *Proc. Natl. Acad. Sci. USA* 82 (1985) 3582–3585.
- [60] S. Vijay-Kumar, C.E. Bugg, W.J. Cook, Structure of ubiquitin refined at 1.8 Angstrom resolution, *J. Mol. Biol.* 194 (1987) 531–544.
- [61] L.K. Steinrauf, Preliminary X-ray data for some new crystalline forms of beta-lactoglobulin and hen egg-white lysozyme, *Acta Crystallogr.* 12 (1959) 77–79.
- [62] M.M. Ries-Kautt, A.F. Ducruix, Relative effectiveness of various ions on the solubility and crystal-growth of lysozyme, *J. Biol. Chem.* 264 (1989) 745–748.
- [63] A.N. Allerhand, R.F. Childers, Studies of individual carbon sites of hen egg white lysozyme by natural abundance carbon-13 nuclear magnetic resonance spectroscopy: assignment of the nonprotonated aromatic carbon resonances to specific residues in the sequence, *J. Biol. Chem.* 252 (1976) 1786–1794.
- [64] A. Pahler, W.A. Hendrickson, M.A.G. Kolks, C.E. Argarana, C.R. Cantor, Characterization and crystallization of core streptavidin, *J. Biol. Chem.* 262 (1987) 13933–13937.
- [65] D.D. Leonidas, R. Shapiro, L.I. Irons, N. Russo, K.R. Acharya, Crystal structures of ribonuclease A complexes with 5'-diphosphadenosine 3'-phosphate and 5'-diphosphoadenine 2'-phosphate at 1.7 Angstrom resolution, *Biochemistry* 36 (1997) 5578–5588.
- [66] R.G. Sanishvili, E. Margoliash, M.L. Westbrook, K.W. Volz, Crystallization of wild-type and mutant ferricytochromes *c* at low ionic strength: seeding technique and X-ray diffraction analysis, *Acta Crystallogr. D* 50 (1994) 687–694.
- [67] E. Oldfield, A. Allerhand, Cytochrome *c*. Observation of numerous single-carbon sites of the reduced and oxidized species by means of natural abundance <sup>13</sup>C nuclear magnetic resonance spectroscopy, *Proc. Natl. Acad. Sci. USA* 70 (1973) 3531–3535.
- [68] E.F. Garman, E.P. Mitchell, Glycerol concentrations required for cryoprotection of 50 typical protein crystallization solutions, *J. Appl. Crystallogr.* 29 (1996) 584–587.
- [69] C.A. Fyfe, H. Strobl, G.T. Kokotailo, G.J. Kennedy, G.E. Barlow, Ultra-high-resolution Si-29 solid-state MAS NMR investigation of sorbate and temperature-induced changes in the lattice structure of zeolite Zsm-5, *J. Am. Chem. Soc.* 110 (1988) 3373–3380.
- [70] D. Vitkup, D. Ringe, G.A. Petsko, M. Karplus, Solvent mobility and the protein glass transition, *Nat. Struct. Biol.* 7 (2000) 34–36.
- [71] A.L. Lee, K.A. Sharp, J.K. Kranz, X.J. Song, A.J. Wand, Temperature dependence of the internal dynamics of a calmodulin-peptide complex, *Biochemistry* 41 (2002) 13814–13825.
- [72] R.B. Von Dreele, P.W. Stephens, G.D. Smith, R.H. Blessing, The first protein crystal structure determined from high-resolution X-ray powder diffraction data: a variant of T3R3 human insulin-zinc complex produced by grinding, *Acta Crystallogr. D* 56 (2000) 1549–1553.
- [73] R.B. Von Dreele, Binding of N-acetylglucosamine to chicken egg lysozyme: a powder diffraction study, *Acta Crystallogr. D* 57 (2001) 1836–1842.